

Phenomenology of pseudotensor mesons and the pseudotensor glueball

Adrian Koenigstein^{1,2}, Francesco Giacosa^{3,1}

¹*Institute for Theoretical Physics, Johann Wolfgang Goethe University,
Max-von-Laue-Str. 1, 60438 Frankfurt am Main, Germany*

²*Frankfurt Institute for Advanced Studies,
Ruth-Moufang-Str. 1, 60438 Frankfurt am Main, Germany*

³*Institute of Physics, Jan Kochanowski University,
ul. Swietokrzyska 15, 25-406 Kielce, Poland*

December 16, 2016

Abstract

We study the decays of the pseudotensor mesons [$\pi_2(1670)$, $K_2(1770)$, $\eta_2(1645)$, $\eta_2(1870)$] interpreted as the ground-state nonet of 1^1D_2 $\bar{q}q$ states using interaction Lagrangians which couple them to pseudoscalar, vector, and tensor mesons. While the decays of $\pi_2(1670)$ and $K_2(1770)$ can be well described, the decays of the isoscalar states $\eta_2(1645)$ and $\eta_2(1870)$ can be brought in agreement with the present experimental data only if the mixing angle between nonstrange and strange states is surprisingly large (about -42° , similar to the mixing in the pseudoscalar sector, in which the chiral anomaly is active). Such a large mixing angle is however at odd with all other conventional quark-antiquark nonets: if confirmed, a deeper study of its origin will be needed in the future. Moreover, the $\bar{q}q$ assignment of pseudotensor states predicts that the ratio $[\eta_2(1870) \rightarrow a_2(1320) \pi]/[\eta_2(1870) \rightarrow f_2(1270) \eta]$ is about 23.5. This value is in agreement with Barberis et al., (20.4 ± 6.6), but disagrees with the recent reanalysis of Anisovich et al., (1.7 ± 0.4). Future experimental studies are necessary to understand this puzzle. If Anisovich's value shall be confirmed, a simple nonet of pseudoscalar mesons cannot be able to describe data (different assignments and/or additional state, such as an hybrid state, will be needed). In the end, we also evaluate the decays of a pseudoscalar glueball into the aforementioned conventional $\bar{q}q$ states: a sizable decay into $K_2^*(1430) K$ and $a_2(1230) \pi$ together with a vanishing decay into pseudoscalar-vector pairs [such as $\rho(770) \pi$ and $K^*(892) K$] are expected. This information can be helpful in future studies of glueballs at the ongoing BESIII and at the future PANDA experiments.

1 Introduction

Most of the light mesons listed in the Particle Data Group (PDG) [1] can be understood as quark-antiquark ($\bar{q}q$) states [2], see also e.g. the review in Ref. [3]. Quark-antiquark mesons, also denoted as conventional mesons, are grouped into nonets. This is a consequence of flavor symmetry, $U_V(3)$: in the limit of equal masses of the light quark flavors u , d , and s , the QCD Lagrangian is invariant under their interchange. In reality, this symmetry is explicitly broken by non-equal bare quark masses, mostly due to the fact that the strange quark s is sizable heavier than the up and down quarks u and d [1].

In the limit of vanishing light quark masses, the QCD Lagrangian exhibits also chiral symmetry, $U_R(3) \times U_L(3)$. Quark-antiquark nonets with equal total angular momentum J but with opposite

parity P are connected by chiral transformations. For instance, scalar (1^3P_0 , $J^{PC} = 0^{++}$) and pseudoscalar mesons (1^1S_0 , $J^{PC} = 0^{-+}$) as well as vector (1^3S_1 , $J^{PC} = 1^{--}$) and axial-vector mesons (1^3P_1 , $J^{PC} = 1^{++}$) are chiral partners, e.g. Ref. [4]. In addition to explicit breaking, chiral symmetry is – even more importantly – also broken spontaneously, $U_R(3) \times U_L(3) \rightarrow U_V(3)$: pseudoscalar mesons (e.g., the pions) are the corresponding quasi-Goldstone bosons.

Tensor mesons (1^3P_2 , $J^{PC} = 2^{++}$) are another example of a very well-understood $\bar{q}q$ nonet: their decays fit nicely into this scheme [2, 5–7]. The chiral partners of tensor mesons, the pseudotensor mesons (1^1D_2 , $J^{PC} = 2^{-+}$), are not so well understood, e.g. Refs. [8, 9] and Refs. therein. The standard assignment [1, 2] contains the isotriplet state $\pi_2(1670)$, the isodoublet states $K_2(1770)$, and the isoscalar states $\eta_2(1645)$ and $\eta_2(1870)$. We plan to study the decays of these resonances in order to test the validity of this assignment and to investigate the mixing in the isoscalar sector. To this end, we build two effective interaction Lagrangians which describe the decays of pseudotensor states into vector-pseudoscalar and into tensor-pseudoscalar pairs. The isotriplet and isodoublet states $\pi_2(1670)$ and $K_2(1770)$ fit well into the $\bar{q}q$ picture. However, in the isoscalar sector the situation is not that simple: the only possible way to understand the experimental results of $\eta_2(1645)$ and $\eta_2(1870)$ listed in the PDG is a very large mixing in the isoscalar-pseudotensor sector. In fact, the mixing angle between the purely nonstrange and strange states turns out to be about -42° in our model, which is very similar to the one in the pseudoscalar sector (leading to the famous mixing among η and $\eta'(958)$, e.g. Ref. [10–12].) However, while the large pseudoscalar-isoscalar mixing is related to the chiral anomaly, such an analogous strong mixing in the pseudotensor sector, if confirmed, would require a careful analysis in order to be understood.

In addition to the mixing angle, in the isoscalar sector there are some conflicting experimental informations about the ratio $[\eta_2(1870) \rightarrow a_2(1320)\pi]/[\eta_2(1870) \rightarrow f_2(1270)\eta]$ that we will discuss. From an experimental point of view it is expected that the GlueX [13–15] and CLAS12 [16] experiment at Jefferson Lab will soon start taking data (photoproduction of mesons by photon-nucleon scattering) and can possibly shed light on pseudotensor states in general, with special attention to the $\eta_2(1870)$ state. Indeed, one of the main motivations of the present work is to draw attention on the existing problems in understanding pseudotensor states. The hope is that new and better experimental data from Jlab will be available in the upcoming years.

Another interesting – although yet only theoretical – pseudotensor state is the pseudotensor glueball. According to lattice QCD its mass is supposed to be about 3 GeV [17, 18]. A simple modification of our interaction Lagrangians allows to make some predictions concerning this putative state. This might help to identify possible glueball candidates.

The article is organized as follows: in Sec. 2 we discuss $\bar{q}q$ nonets, their microscopic currents and quantum numbers; then, we introduce the two effective Lagrangians mentioned above and the corresponding decay widths. In Sec. 3 we present the results for the decays of isotriplet and isodoublet members of the pseudoscalar nonet. In Sec. 4 we turn to the isoscalar sector: after showing that a small mixing angle cannot be correct, we show that a large negative mixing angle allows to understand all the existing data. Within this context, we describe also some puzzling entries in the PDG. In Sec. 5 we concentrate on the decays of a (yet hypothetical) pseudoscalar glueball. Finally, in Sec. 6 we turn to the conclusions and outlooks.

2 The model

In this Section we describe the model for the decays of pseudotensor mesons. First, we introduce the relevant quark-antiquark nonets and provide a brief repetition of some aspects of the quark-antiquark assignments. In the second step, the effective Lagrangians for the present model are presented.

2.1 Quark-antiquark nonets

The underlying structure of conventional meson fields is described via $\bar{q}q$ currents. First, we briefly review their quantum numbers and illustrate their construction scheme.

The total spin of a $\bar{q}q$ bound state can be either $S = 0$ or $S = 1$, whereas the angular momentum is not limited: $L = 0$ (ground state), $1, 2, 3, \dots$. The total angular momentum $\vec{J} = \vec{L} + \vec{S}$ is restricted by $|L - S| \leq J \leq L + S$. Parity and charge conjugation quantum numbers are given by

$$P = (-1)^{L+1}, \quad C = (-1)^{L+S}, \quad (2.1)$$

(where – strictly speaking – only diagonal members of a given multiplet are C -eigenstates). As usual, mesons are grouped into nonets (see below) corresponding to a well-defined combination J^{PC} [1]. In Tab. (1) we present various combinations J^{PC} together with the values of L, S , the old spectroscopic notation $n^{2S+1}L_J$, and the corresponding microscopic currents generating them (here, the quark fields reads q_i , where $i \in \{u, d, s\}$). We recall that n is the radial quantum number ($n = 1$ for all the cases under considerations), $L = S, P, D, \dots$, and $\overleftrightarrow{\partial}_\mu = \overrightarrow{\partial}_\mu - \overleftarrow{\partial}_\mu$.

Meson	$n^{2S+1}L_J$	J^{PC}	S	L	Hermitian quark current operators
pseudoscalar	1^1S_0	0^{-+}	0	0	$P_{ij} = \bar{q}_j i \gamma^5 q_i$
vector	1^3S_1	1^{--}	1		$V_{ij}^\mu = \bar{q}_j \gamma^\mu q_i$
pseudovector	1^1P_1	1^{+-}	0	1	$P_{ij}^\mu = \bar{q}_j \gamma^5 \overleftrightarrow{\partial}^\mu q_i$
scalar	1^3P_0	0^{++}	1		$S_{ij} = \bar{q}_j q_i$
axial vector	1^3P_1	1^{++}	1		$A_{ij}^\mu = \bar{q}_j \gamma^5 \gamma^\mu q_i$
tensor	1^3P_2	2^{++}	1		$X_{ij}^{\mu\nu} = \bar{q}_j i \left[\gamma^\mu \overleftrightarrow{\partial}^\nu + \gamma^\nu \overleftrightarrow{\partial}^\mu - \frac{2}{3} \tilde{G}^{\mu\nu} \overleftrightarrow{\not{\partial}} \right] q_i$
pseudotensor	1^1D_2	2^{-+}	0	2	$T_{ij}^{\mu\nu} = \bar{q}_j i \left[\gamma^5 \overleftrightarrow{\partial}^\mu \overleftrightarrow{\partial}^\nu - \frac{2}{3} \tilde{G}^{\mu\nu} \overleftrightarrow{\partial}_\alpha \overleftrightarrow{\partial}^\alpha \right] q_i$
excited vector	1^3D_1	1^{--}	1		$S_{ij}^\mu = \bar{q}_j \overleftrightarrow{\partial}^\mu q_i$
axial tensor	1^3D_2	2^{--}	1		$B_{ij}^{\mu\nu} = \bar{q}_j i \left[\gamma^5 \gamma^\mu \overleftrightarrow{\partial}^\nu + \gamma^5 \gamma^\nu \overleftrightarrow{\partial}^\mu - \frac{2}{3} \tilde{G}^{\mu\nu} \gamma^5 \overleftrightarrow{\not{\partial}} \right] q_i$
spin-3 tensor	1^3D_3	3^{--}	1		\dots

Table 1: Types of different mesons and their corresponding quantum numbers. We use the projector $\tilde{G}^{\mu\nu} = \eta^{\mu\nu} - \frac{k^\mu k^\nu}{k^2}$.

We now introduce the matrices of the nonets relevant in the present work. The nonet of pseudoscalar mesons is given by

$$P = \begin{pmatrix} \frac{\eta_N + \pi^0}{\sqrt{2}} & \pi^+ & K^+ \\ \pi^- & \frac{\eta_N - \pi^0}{\sqrt{2}} & K^0 \\ K^- & \bar{K}^0 & \eta_S \end{pmatrix}, \quad (2.2)$$

where $\eta_N = \sqrt{1/2}(\bar{u}u + \bar{d}d)$ is the pure non-strange state and $\eta_S = \bar{s}s$ the pure strange state. The identifications of the fields with physical resonances are listed in Tab. (2), while the transformation properties under parity, charge conjugation, and flavor transformations are reported in Tab. (3). The isoscalar mixing angle $\beta_p = -40.5^\circ$ in the non-strange-strange pseudoscalar sector is taken from [10]. The large maxing is linked to the chiral anomaly, see e.g. Refs. [3, 4, 11].

Physical resonances	Nonet $q\bar{q}$ -states
π	π
K	K
η	$\eta_N \cos \beta_p + \eta_S \sin \beta_p$
$\eta'(958)$	$-\eta_N \sin \beta_p + \eta_S \cos \beta_p$
$\rho(770)$	ρ
$K^*(892)$	K^*
$\omega(782)$	$\omega_N \cos \beta_v + \omega_S \sin \beta_v$
$\phi(1020)$	$-\omega_N \sin \beta_v + \omega_S \cos \beta_v$
$a_2(1320)$	a_2
$K_2^*(1430)$	K_2^*
$f_2(1270)$	$f_{2,N} \cos \beta_t + f_{2,S} \sin \beta_t$
$f_2'(1525)$	$-f_{2,N} \sin \beta_t + f_{2,S} \cos \beta_t$
$\pi_2(1670)$	π_2
$K_2(1770)$	K_2
$\eta_2(1645)$	$\eta_{2,N} \cos \beta_{pt} + \eta_{2,S} \sin \beta_{pt}$
$\eta_2(1870)$	$-\eta_{2,N} \sin \beta_{pt} + \eta_{2,S} \cos \beta_{pt}$

Table 2: Assignment of physical resonances to $\bar{q}q$ -states in the model.

Similarly, vector mesons are arranged in the vector nonet given by

$$V^\mu = \begin{pmatrix} \frac{\omega_N^\mu + \rho^{0\mu}}{\sqrt{2}} & \rho^{+\mu} & K^{*+\mu} \\ \rho^{-\mu} & \frac{\omega_N^\mu - \rho^{0\mu}}{\sqrt{2}} & K^{*0\mu} \\ K^{*-\mu} & \bar{K}^{*0\mu} & \omega_S^\mu \end{pmatrix}, \quad (2.3)$$

where ω_N is purely non-strange and ω_S purely strange. Identifications and transformation properties are provided by Tab. (2) and Tab. (3). The isoscalar-vector mixing angle is very small: $\beta_v = -3.8^\circ$ [1]. The physical states ω and ϕ are dominated by non-strange and strange components, respectively.

We now turn to tensor and pseudotensor states (for a recent review on mathematical aspects of tensor fields, see Ref. [19] and references therein). The tensor meson nonet reads

$$X^{\mu\nu} = \begin{pmatrix} \frac{f_{2,N}^{\mu\nu} + a_2^{0\mu\nu}}{\sqrt{2}} & a_2^{+\mu\nu} & K_2^{*+\mu\nu} \\ a_2^{-\mu\nu} & \frac{f_{2,N}^{\mu\nu} - a_2^{0\mu\nu}}{\sqrt{2}} & K_2^{*0\mu\nu} \\ K_2^{*- \mu\nu} & \bar{K}_2^{*0\mu\nu} & f_{2,S}^{\mu\nu} \end{pmatrix}. \quad (2.4)$$

In analogy to the vector case, the mixing angle between the pure non-strange $f_{2,N}$ and the pure strange $f_{2,S}$ is small: $\beta_t = 3.2^\circ$, see Ref. [1]. Finally, the nonet of pseudotensor states – which constitutes the main subject of the present work – is given by

$$T^{\mu\nu} = \begin{pmatrix} \frac{\eta_{2,N}^{\mu\nu} + \pi_2^{0\mu\nu}}{\sqrt{2}} & \pi_2^{+\mu\nu} & K_2^{+\mu\nu} \\ \pi_2^{-\mu\nu} & \frac{\eta_{2,N}^{\mu\nu} - \pi_2^{0\mu\nu}}{\sqrt{2}} & K_2^{0\mu\nu} \\ K_2^{-\mu\nu} & \bar{K}_2^{0\mu\nu} & \eta_{2,S}^{\mu\nu} \end{pmatrix}, \quad (2.5)$$

see again Tab. (2) and Tab. (3) for the physical content and transformations of (pseudo)tensor mesons.

The mixing angle β_{pt} is – at first – unknown. Naively, one would expect a small mixing angle (similarly to the vector and the tensor mesons; alternatively, one may use the Okubo formula, which yields $\beta_{pt} \approx 14.8^\circ$ derived from (15.9) in [1]). However, a small mixing angle does not lead to acceptable results within our model. A large and negative mixing angle – as in the pseudoscalar sector – is needed, see Sec. 4.

Other mesonic nonets can be constructed in the same way, see for instance Refs. [4, 20, 21]. They are omitted here, since they do not enter the decays under consideration.

Nonet	Parity (P)	Charge conjugation (C)	Flavour ($U_V(3)$)
P	$-P(t, -\vec{x})$	P^t	UPU^\dagger
V^μ	$V_\mu(t, -\vec{x})$	$-(V^\mu)^t$	$UV^\mu U^\dagger$
$X^{\mu\nu}$	$X_{\mu\nu}(t, -\vec{x})$	$(X^{\mu\nu})^t$	$UX^{\mu\nu}U^\dagger$
$T^{\mu\nu}$	$-T_{\mu\nu}(t, -\vec{x})$	$(T^{\mu\nu})^t$	$UT^{\mu\nu}U^\dagger$

Table 3: Transformation properties of the pseudoscalar (2.2), the vector (2.3), the tensor (2.4), and pseudotensor (2.5) nonets under charge conjugation C , parity P , and flavour transformations $U_V(3)$. Notice the position of the Lorentz indices for parity transformations, since spatial and time-like indices do not transform identically.

2.2 The interaction Lagrangians and tree-level decay width

Using the nonets (2.2) - (2.5) introduced in the previous subsection, we construct two effective interaction Lagrangians which describe the decays of pseudotensor mesons.

The first Lagrangian \mathcal{L}_{TVP} includes the coupling of pseudotensor mesons to vector-pseudoscalar pairs,

$$\mathcal{L}_{TVP} = c_{TVP} \text{Tr}\{T_{\mu\nu}[V^\mu, (\partial^\nu P)]_-\}, \quad (2.6)$$

where c_{TVP} denotes an (at first) unknown dimensionless coupling constant and $[\cdot]_-$ is the commutator.

The second interaction Lagrangian \mathcal{L}_{TXP} contains the coupling of pseudotensor mesons to tensor-pseudoscalar pairs,

$$\mathcal{L}_{TXP} = c_{TXP} \text{Tr}(T_{\mu\nu}\{X^{\mu\nu}, P\}_+), \quad (2.7)$$

where c_{TXP} is an (at first) unknown coupling constant with dimension energy and $\{\cdot\}_+$ is the anti-commutator.

Both Lagrangians are invariant under CPT -, Poincaré- and flavour-transformations listed in Tab. (3). The explicit form of the Lagrangians are presented in App. A. Hence, the total Lagrangian, which specifies our model, is given by

$$\mathcal{L}_{T\text{-total}} = \mathcal{L}_{\text{kin}} + \mathcal{L}_{TVP} + \mathcal{L}_{TXP}, \quad (2.8)$$

where $\mathcal{L}_{\text{kin}} = \frac{1}{2} \text{Tr}[(\partial_\mu P)(\partial^\mu P)] + \dots$ contains the usual kinetic terms of all relevant nonets (for the tensor fields, see again Ref. [19]), while the interaction term is the sum of the two interaction Lagrangians presented above.

The interaction Lagrangians outlined above can be considered as the dominant terms in the large- N_c and flavour breaking expansions. For instance, the full Lagrangian for the interaction of the pseudotensor field with tensor and pseudoscalar field takes the form

$$\begin{aligned}\mathcal{L}_{TXP}^{full} = & c_{TXP} \text{Tr}(T_{\mu\nu}\{X^{\mu\nu}, P\}_+) + c_{TXP} \text{Tr}(\hat{\delta} T_{\mu\nu}\{X^{\mu\nu}, P\}_+) + \\ & + \tilde{c}_{TXP} \text{Tr}(T_{\mu\nu}) \text{Tr}(\{X^{\mu\nu}, P\}_+) + \tilde{c}_{TXP} \text{Tr}(\hat{\delta} T_{\mu\nu}) \text{Tr}(\{X^{\mu\nu}, P\}_+) + \dots\end{aligned}\quad (2.9)$$

where the matrix $\hat{\delta} = \text{diag}(0, \delta_d, \delta_s)$ describes isospin violation. Following [22] and denoting V as the potential responsible of the creation of a quark-antiquark pair from the QCD vacuum, we find,

$$\begin{aligned}\delta_d &= \frac{\langle 0|V|\bar{d}d\rangle}{\langle 0|V|\bar{u}u\rangle} - 1 \simeq 0 \quad (\text{isospin violation can be neglected to a very good level of accuracy}), \\ \delta_s &= \frac{\langle 0|V|\bar{s}s\rangle}{\langle 0|V|\bar{u}u\rangle} - 1 \lesssim 0.2 \quad (\text{small but eventually important for a precise description}).\end{aligned}$$

A similar value for δ_s has been obtained in Refs. [2, 23]. Moreover, according to Refs. [24–26] we expect

$$c_{TXP} \propto N_c^{-1/2}, \quad (2.10)$$

$$\tilde{c}_{TXP} \propto N_c^{-3/2}. \quad (2.11)$$

The first term in Eq. (2.9) is the dominant one: due to the present experimental status this is the only term in the pseudotensor-tensor-pseudoscalar sector which is used in the numerical calculations of the present work. Then, the second and the third term of Eq. (2.9) generate decay amplitudes proportional to $c_{TXP} \delta_s$ and \tilde{c}_{TXP} respectively, hence they generate corrections of the order of 5-10%, which should be taken into account when better experimental data will be available. Further terms such as the fourth term generate a contribution of the type $\tilde{c}_{TXP} \delta_s$, hence they are suppressed twice, because of large- N_c and flavour symmetry violation. Their influence is expected to be about 1%, hence negligible.

For what concerns the interaction term of pseudotensor mesons with pseudoscalar and vector fields the expansion is similar:

$$\begin{aligned}\mathcal{L}_{TVP}^{full} = & c_{TVP} \text{Tr}\{T_{\mu\nu}[V^\mu, (\partial^\nu P)]_-\} + c_{TVP} \text{Tr}\{\hat{\delta} T_{\mu\nu}[V^\mu, (\partial^\nu P)]_-\} \\ & + \tilde{c}_{TVP} \text{Tr}\{\hat{\delta} T_{\mu\nu}\} \text{Tr}\{\hat{\delta} [V^\mu, (\partial^\nu P)]_-\} + \dots\end{aligned}\quad (2.12)$$

As before, the first term dominates and the only term of Eq. (2.12) considered in this paper. There is however a difference between Eq. (2.9) and Eq. (2.12): due to the anti-commutator in the latter, some terms do not appear in the expansion. The next-to-leading contribution is the second term $\propto c_{TVP} \delta_s$ (breaking of flavour symmetry). Furthermore, one has terms $\propto \tilde{c}_{TVP} \delta_s$ such as the third one which suppressed in N_c and the flavour expansions.

We now turn to the tree-level decay widths. The tree-level decay widths derived from the two Lagrangians \mathcal{L}_{TVP} and \mathcal{L}_{TXP} read

$$\Gamma_{T \rightarrow VP}^{tl}(m_T, m_V, m_P) = \frac{k_f}{8\pi m_T} \frac{g_{TVP}^2}{15} \left(2 \frac{k_f^4}{m_V^2} + 5 k_f^2 \right) \Theta(m_T - m_V - m_P), \quad (2.13)$$

and

$$\Gamma_{T \rightarrow XP}^{tl}(m_T, m_X, m_P) = \frac{k_f}{8\pi m_T} \frac{g_{TXP}^2}{45} \left(4 \frac{k_f^4}{m_X^4} + 30 \frac{k_f^2}{m_X^2} + 45 \right) \Theta(m_T - m_X - m_P). \quad (2.14)$$

Above, m_T is the mass of a (decaying) pseudotensor fields, while m_V , m_P , and m_X are the masses of the vector, pseudoscalar, and tensor states (the decay products). $\Theta(x)$ denotes the Heaviside step-function. The quantities g_{TVP} and g_{TXP} , which are proportional to the coupling constants c_{TVP} and c_{TXP} , have to be calculated for each decay channel separately by using the expressions in App. A. Finally, the function $k_f \equiv k_f(m_T, m_V, m_P)$ is the modulus of the momentum \vec{k}_f of one of the outgoing particles. Its analytic expression in Eq. (2.13) reads:

$$k_f(m_T, m_V, m_P) = \frac{1}{2m_T} \sqrt{m_T^4 + (m_V^2 - m_P^2)^2 - 2m_T^2(m_V^2 + m_P^2)}, \quad (2.15)$$

while its expression in Eq. (2.14) is obtained by substituting $m_V \rightarrow m_X$.

These decay widths (2.13) and (2.14) are derived via Feynman rules under the use of the polarization vectors (tensors) and their corresponding completeness relations. For a derivation of the unpolarized invariant decay amplitudes see App. B.

Calculations are performed at tree-level, that is NLO effects due to quantum loops are not considered here. Loops are expected to be small when the ratio $\Gamma/(M - M_{th})$ is sufficiently small (≤ 0.2 , where Γ and M are the decay width and the mass of the decaying state and M_{th} is the lowest threshold [27]). This condition is fulfilled for the pseudotensor mesons under study.

3 Results for $\pi_2(1670)$ and $K_2(1770)$

As a first step, we determine the coupling constants c_{TVP} and c_{TXP} using two – well known – experimental decay widths,

$$\pi_2(1670) \rightarrow \rho(770) \pi, \quad \text{and} \quad \pi_2(1670) \rightarrow f_2(1270) \pi. \quad (3.1)$$

Taking into account that for these two decays one has $g_{TVP}^2 = 2(\sqrt{2}c_{TVP})^2$ and $g_{TXP}^2 = 2 \cos \beta_t c_{TXP}^2$, the use of Eqs. (2.13), (2.14), and (A.1) implies that [see Tab. (4)],

$$c_{TVP}^2 = 11.9 \pm 1.6, \quad c_{TXP}^2 = (15.1 \pm 1.0) \cdot 10^6 \text{ MeV}^2. \quad (3.2)$$

The quoted errors are solely determined by the experimental errors on the decay widths (mass errors are small and negligible for our accuracy).

Once the coupling constants are known, all the isotriplet and isodoublet decays of pseudotensor states are uniquely fixed. The results are shown in Tab. (4).

Decay process	Theory (MeV)	Experiment (MeV)
$\pi_2(1670) \rightarrow \rho(770) \pi$	80.6 ± 10.8	80.6 ± 10.8
$\pi_2(1670) \rightarrow f_2(1270) \pi$	146.4 ± 9.7	146.4 ± 9.7
$\pi_2(1670) \rightarrow \bar{K}^*(892) K + c.c.$	11.7 ± 1.6	10.9 ± 3.7
$\pi_2(1670) \rightarrow \bar{K}_2^*(1430) K + c.c.$	0	
$\pi_2(1670) \rightarrow f_2'(1525) \pi$	0.1 ± 0.1	
$\pi_2(1670) \rightarrow a_2(1320) \pi$	0	not seen
$\pi_2(1670) \rightarrow a_2(1320) \eta$	0	
$\pi_2(1670) \rightarrow a_2(1320) \eta'(958)$	0	
$K_2(1770) \rightarrow \rho(770) K$	22.2 ± 3.0	
$K_2(1770) \rightarrow \bar{K}^*(892) \pi$	25.5 ± 3.4	seen
$K_2(1770) \rightarrow \bar{K}^*(892) \eta$	10.5 ± 1.4	
$K_2(1770) \rightarrow \bar{K}^*(892) \eta'(958)$	0	
$K_2(1770) \rightarrow \omega(782) K$	8.3 ± 1.1	seen
$K_2(1770) \rightarrow \phi(1020) K$	4.2 ± 0.6	seen
$K_2(1770) \rightarrow a_2(1320) K$	0	
$K_2(1770) \rightarrow \bar{K}_2^*(1430) \pi$	84.5 ± 5.6	dominant
$K_2(1770) \rightarrow \bar{K}_2^*(1430) \eta$	0	
$K_2(1770) \rightarrow \bar{K}_2^*(1430) \eta'(958)$	0	
$K_2(1770) \rightarrow f_2(1270) K$	5.8 ± 0.4	seen
$K_2(1770) \rightarrow f_2'(1525) K$	0	

Table 4: Decays of $I = 1$ and $I = 1/2$ pseudotensor states. The first two entries were used to determine the coupling constants of the model, see Eq. (3.2). The total decay widths are $\Gamma_{\pi_2(1670)}^{\text{tot}} = (260 \pm 9) \text{ MeV}$ and $\Gamma_{K_2(1770)}^{\text{tot}} = (186 \pm 14) \text{ MeV}$.

Following comments are in order:

1. We recall that the first two entries of Tab. (4) were used to calculate the coupling constants of the model, see Eq. (3.2). These values are extracted from the PDG using the branching ratio quoted by the PDG: $56.3 \pm 3.2\%$ for $\pi_2(1670) \rightarrow f_2(1270) \pi$ and $31 \pm 4\%$ for $\pi_2(1670) \rightarrow \rho \pi$. However, a closer inspection of the performed experiments on the resonance $\pi_2(1670)$ shows that new experiments are needed to improve experimental knowledge. For instance, the ratio $\Gamma(\rho \pi)/[0.565 \Gamma(f_2(1270) \pi)]$, whose PDG quoted average is 0.97 ± 0.09 , was determined only by two distinct results: $0.76 \pm 0.07 \pm 0.10$ by [28] and 1.01 ± 0.05 by [29]. While consistent among each other, a new experimental determination would be very welcome for our theoretical approach, since the determination of the coupling constant follows from these experimental values.
2. The prediction for the decay channel $\pi_2(1670) \rightarrow \bar{K}^*(892) K$ is in agreement with the present value quoted by the PDG. However, it should be stressed that this value is extracted from a single experiment [30]: a new experimental determination of this quantity is then compelling for a better comparison.
3. In our model $\pi_2(1670)$ does not couple to the $a_2(1320) \pi$ channel, see Eq. (A.2). Experimentally this decay could also be excluded to a good accuracy (for more experimental details see Ref. [31]).
4. The experimental total decay width of $\pi_2(1670)$ reads $\Gamma_{\pi_2(1670)}^{\text{exp,tot}} = (260 \pm 9) \text{ MeV}$. The value in our model is $\approx 238.8 \text{ MeV}$. The reason why the sum of the theoretical and experimental decay modes in our model is slightly smaller than the experimental total width is due to the fact that the model does not include the decay $\pi_2(1670) \rightarrow f_0(500) \pi$, which is $\approx 26 \text{ MeV}$.

(Other channels, which are not present in our model, would also contribute. Nevertheless they are negligibly small [1]). Taking this into account, the model is consistent with the total width.

5. Experimentally, the decay channel $K_2(1770) \rightarrow \bar{K}_2^*(1430) \pi$ is dominant. The total decay width of $K_2(1770)$ is $\Gamma_{K_2(1770)}^{\text{exp,tot}} = (186 \pm 14)$ MeV. Theoretically, the $K_2(1770) \rightarrow \bar{K}_2^*(1430) \pi$ decay mode is the dominant one (84.5 ± 5.6 MeV).
6. The full theoretical decay width of $K_2(1770)$ amounts to (162.0 ± 15.4) MeV which is compatible with the experimental value.
7. Various branching ratios of $K_2(1770)$ can be calculated from Tab. (4). At present, experimental results are missing (no average or fit is quoted by PDG [1]). In this respect, our approach makes predictions for new future experimental measurements. In this context, it will also be possible to determine the mixing angle of the bare 1^1D_2 and 1^3D_2 configurations into the physical $K_2(1770)$ and $K_2(1820)$ states [so far, $K_2(1770)$ is dominated by 1^1D_2].
8. Most of the decays which are predicted by our model to vanish were consistently not seen in experiments. Yet, the decays $\pi_2(1670) \rightarrow a_2(1230) \eta$ and $K_2(1270) \rightarrow K^*(892) \eta$ are expected to be small but not zero. They were not yet measured, hence they represent a test of our approach as soon as new experimental data will be available.

4 The Isoscalar sector: $\eta_2(1645)$ and $\eta_2(1870)$

In this section we present the results of the isoscalar sector of the pseudotensor mesons. In Subsec. 4.1 we show that a small mixing of $\eta_{2,N}$ and $\eta_{2,S}$ is not capable to describe the data. Thus, in Subsec. 4.2 we allow for a large mixing angle: a value of about -40° turns out to be favored. In Subsec. 4.3 we discuss the experimental status of branching ratios with particular attention to $[\eta_2(1870) \rightarrow a_2(1320) \pi] / [\eta_2(1870) \rightarrow f_2(1270) \eta]$, for which conflicting experimental results exist.

4.1 Small strange-nonstrange mixing angle

First, we present the results of the decay widths of the isoscalar $I = 0$ pseudotensor states in Tab. (5) for a vanishing mixing angle ($\beta_{pt} = 0^\circ$) and for a small but non-vanishing angle ($\beta_{pt} = 14.8^\circ$, obtained via the Okubo formula [1]). Both cases lead to inconsistent results. In fact, the decay $\eta_2(1645) \rightarrow a_2(1320) \pi$ turns out to be larger than 300 MeV, which is not acceptable, since it is sizable larger than the total experimental width $\Gamma_{\eta_2(1645)}^{\text{exp,tot}} = (181 \pm 11)$ MeV. These results hold for any small mixing angle ($|\beta_{pt}| \lesssim 30^\circ$).

Decay process	Theory (MeV) ($\beta_{pt} = 14.8^\circ$)	Theory (MeV) ($\beta_{pt} = 0.0^\circ$)	Experiment (MeV)
$\eta_2(1645) \rightarrow \bar{K}^*(892) K + c.c.$	3.2 ± 0.4	8.6 ± 1.1	seen
$\eta_2(1645) \rightarrow a_2(1320) \pi$	315.6 ± 21.2	337.8 ± 22.6	
$\eta_2(1645) \rightarrow \bar{K}_2^*(1430) K + c.c.$	0	0	
$\eta_2(1645) \rightarrow f_2(1270) \eta$	0	0	not seen
$\eta_2(1645) \rightarrow f_2(1270) \eta'(958)$	0	0	
$\eta_2(1645) \rightarrow f_2'(1525) \eta$	0	0	
$\eta_2(1645) \rightarrow f_2'(1525) \eta'(958)$	0	0	
$\eta_2(1870) \rightarrow \bar{K}^*(892) K + c.c.$	60.1 ± 8.0	45.6 ± 6.1	
$\eta_2(1870) \rightarrow a_2(1320) \pi$	32.2 ± 2.1	0	
$\eta_2(1870) \rightarrow \bar{K}_2^*(1430) K + c.c.$	0	0	
$\eta_2(1870) \rightarrow f_2(1270) \eta$	2.5 ± 0.2	0.1 ± 0.1	
$\eta_2(1870) \rightarrow f_2(1270) \eta'(958)$	0	0	
$\eta_2(1870) \rightarrow f_2'(1525) \eta$	0	0	
$\eta_2(1870) \rightarrow f_2'(1525) \eta'(958)$	0	0	

Table 5: Decays of $I = 0$ pseudo-tensor states. The total decay widths are $\Gamma_{\eta_2(1645)}^{\text{tot}} = (181 \pm 11)$ MeV and $\Gamma_{\eta_2(1870)}^{\text{tot}} = (225 \pm 14)$ MeV.

In addition, the following comments are in order:

1. The PDG reports the following ratios for $\eta_2(1645)$:

$$\Gamma^{\text{exp}}(\bar{K} K \pi) / \Gamma^{\text{exp}}(a_2(1320) \pi) = 0.07 \pm 0.03, \quad (4.1)$$

$$\Gamma^{\text{exp}}(a_2(1320) \pi) / \Gamma^{\text{exp}}(a_0(980) \pi) = 13.1 \pm 2.3. \quad (4.2)$$

Thus, the channel $\eta_2(1645) \rightarrow a_2(1320) \pi$ is indeed expected to be dominant. This fact is well captured by the theoretical results of Tab. (5), which however overshoot the data. Moreover, the experiment shows that $\Gamma^{\text{exp}}(\bar{K} K \pi) \ll \Gamma^{\text{exp}}(a_2(1320) \pi)$: this feature is in agreement with the experiment upon identifying $\bar{K} K \pi \approx \bar{K}^*(892) K + c.c.$.

2. For what concerns $\eta_2(1870)$, the PDG reports $\Gamma^{\text{exp}}(a_2(1320) \pi) / \Gamma^{\text{exp}}(f_2(1270) \eta) = 1.7 \pm 0.4$, i.e. nonzero. This result excludes $\beta_{pt} = 0.0^\circ$ (for which the theoretical ratio would vanish). Yet, for $\beta_{pt} = 14.8^\circ$ a large ratio is obtained (≈ 12). However, while all experiments do agree that this ratio is sizable, there is a clear disagreement on its actual magnitude. In the next two subsections [(4.2) and (4.3)] we describe this issue in detail.
3. For what concerns $K^*(892)K + c.c.$ of $\eta_2(1870)$, there is also a disagreement with the theoretical results of Tab. (5) and the experiment. Namely, the theoretical predictions are large. This is understandable, because for a small β_{pt} the resonance $\eta_2(1870)$ is dominated by its $\bar{s}s$ component. However, the kaonic channel has not been seen in the experiments. Also this aspect is analyzed in the upcoming subsection.

In conclusion, various inconsistencies with experimental data exist: a small mixing angle must be rejected.

4.2 Large strange-nonstrange mixing angle

Models based on mesonic $\bar{q}q$ nonets and flavour symmetry have proven to be successful, as the clear example of tensor mesons shows [5]. Yet, the results of the previous section shows that the

case of pseudotensor mesons is more complicated than expected. As an immediate next step, we leave the mixing angle β_{pt} unconstrained and test if there is an – even large – value which allows for a correct description of all known experimental data.

In Fig. (1), upper panel, we plot the theoretical decay widths $\eta_2(1645) \rightarrow a_2(1320) \pi$ and $\eta_2(1870) \rightarrow a_2(1320) \pi$ as a function of β_{pt} . Only for $\beta_{pt} \approx \pm 40^\circ$ the theoretical decay of $\eta_2(1645)$ and $\eta_2(1870)$ are comparable with the corresponding total experimental widths. Namely, for values of $\beta_{pt} \in [-40^\circ, +40^\circ]$ the decay $\eta_2(1645) \rightarrow a_2(1320) \pi$ exceeds clearly the total decay width of $\eta_2(1645)$ [which is constrained experimentally to be (181 ± 11) MeV], while for $\beta_{pt} \in [-90^\circ, -45^\circ] \cup [+45^\circ, +90^\circ]$ the decay $\eta_2(1645) \rightarrow a_2(1320) \pi$ exceeds the total decay width of $\eta_2(1870)$ [which is given experimentally by (225 ± 14) MeV]. Hence, a large mixing angle $\beta_{pt} \approx \pm 40^\circ$ is a necessary condition for a consistent description of data.

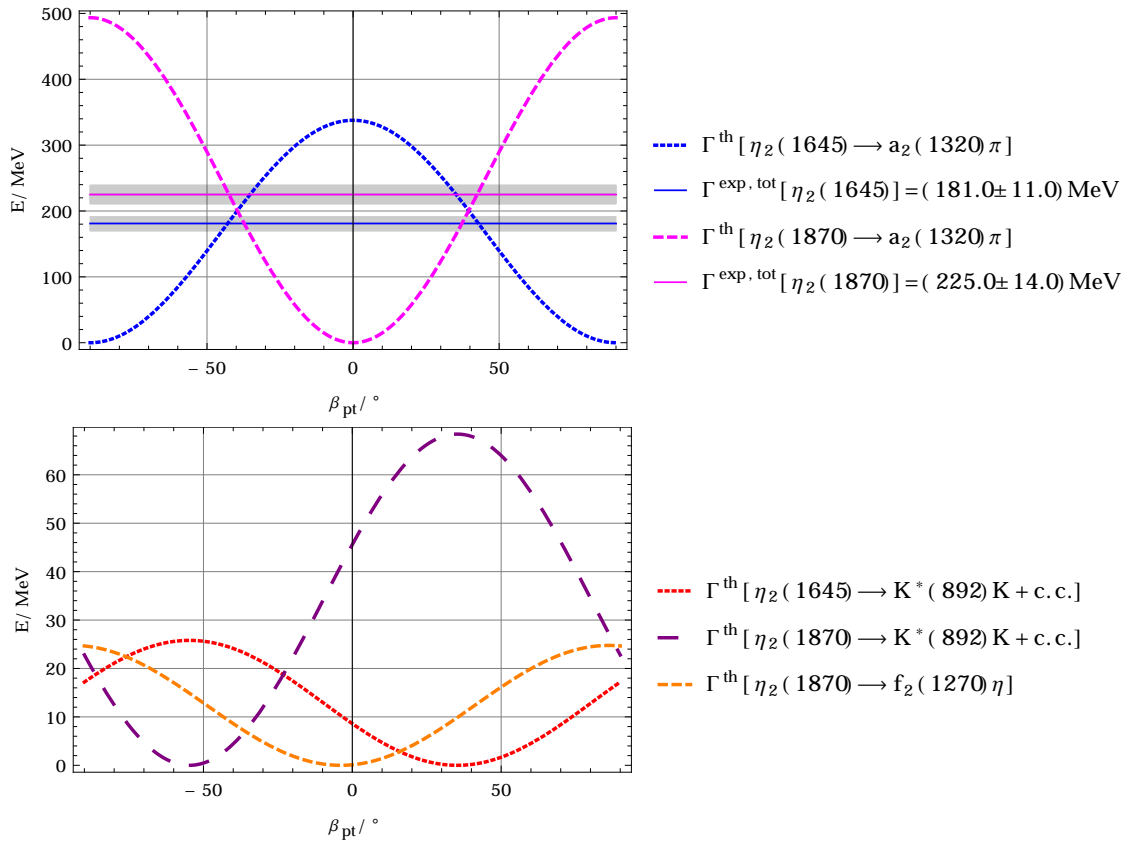


Figure 1: Upper panel: $\eta_2(1645) \rightarrow a_2(1320) \pi$ and $\eta_2(1870) \rightarrow a_2(1320) \pi$ as function of β_{pt} . The bands correspond to the total decay widths of $\eta_2(1645)$ and $\eta_2(1870)$. Lower panel: $\eta_2(1645) \rightarrow K^*(892) K$, $\eta_2(1870) \rightarrow K^*(892) K$, and $\eta_2(1870) \rightarrow f_2(1270) \eta$ as function of β_{pt} . Only for $\beta_{pt} \approx -40^\circ$ the decay $\eta_2(1870) \rightarrow K^*(892) K$ is suppressed. For further details, see discussion in the main text.

In Fig. (1), lower panel, we show three further decay channels as function of β_{pt} : $\eta_2(1645) \rightarrow K^*(892) K$, $\eta_2(1870) \rightarrow K^*(892) K$, and $\eta_2(1870) \rightarrow f_2(1270) \eta$. In particular, the channel $\eta_2(1870) \rightarrow K^*(892) K$ is crucial for our purposes: a negative and large mixing angle, $\beta_{pt} \approx (-40^\circ, -50^\circ)$, is needed to obtain a small partial decay width (this is a consequence of destructive interference). This is necessary to be in agreement with the fact that this decay channel has not been seen in experiments.

Combining the results of both panels, we realize that a large and negative mixing angle is the

only possibility. It is instructive to make a definite choice: this is done in Tab. (6) for the illustrative value $\beta_{pt} = -42^\circ$. It is visible that all theoretical results are in good agreement with the experimental data.

Decay process	Theory (MeV) ($\beta_{pt} = -42^\circ$)	Experiment (MeV)
$\eta_2(1645) \rightarrow \bar{K}^*(892) K + c.c.$	24.7	seen
$\eta_2(1645) \rightarrow a_2(1320) \pi$	186.5	
$\eta_2(1645) \rightarrow \bar{K}_2^*(1430) K + c.c.$	0	
$\eta_2(1645) \rightarrow f_2(1270) \eta$	0	not seen
$\eta_2(1645) \rightarrow f_2(1270) \eta'(958)$	0	
$\eta_2(1645) \rightarrow f_2'(1525) \eta$	0	
$\eta_2(1645) \rightarrow f_2'(1525) \eta'(958)$	0	
$\eta_2(1870) \rightarrow \bar{K}^*(892) K + c.c.$	3.3	
$\eta_2(1870) \rightarrow a_2(1320) \pi$	221.0	
$\eta_2(1870) \rightarrow \bar{K}_2^*(1430) K + c.c.$	0	
$\eta_2(1870) \rightarrow f_2(1270) \eta$	9.4	
$\eta_2(1870) \rightarrow f_2(1270) \eta'(958)$	0	
$\eta_2(1870) \rightarrow f_2'(1525) \eta$	0	
$\eta_2(1870) \rightarrow f_2'(1525) \eta'(958)$	0	

Table 6: Decays of $I = 0$ pseudotensor states. The total decay widths are $\Gamma_{\eta_2(1645)}^{\text{tot}} = (181 \pm 11)$ MeV and $\Gamma_{\eta_2(1870)}^{\text{tot}} = (225 \pm 14)$ MeV.

Some additional remarks are in order:

1. Our model is based on exact flavour symmetry and only large- N_c dominant terms are retained. An agreement at the 5–10% level is expected. In order to achieve a better precision, one should include further terms (see above).
2. The experimental total width of $\eta_2(1645)$ is (181 ± 11) MeV, while the theoretical result for $\beta_{pt} = -42^\circ$ reads 211 MeV [from Tab. (6)]. Taking into account the uncertainty on the coupling constant (keeping $\beta_{pt} = -42^\circ$ fixed), one obtains (211.2 ± 13) MeV. Obviously, this is only an underestimation of the full error, but it shows that theory and experiment are compatible. The use of remark (1) would improve the agreement.
3. The experimental total width of $\eta_2(1870)$ is (225 ± 14) MeV; the corresponding theoretical width for $\beta_{pt} = -42^\circ$ reads 233.7 MeV. Including errors on the coupling constants implies (233.7 ± 15) MeV. Also in this case, there is agreement of theory and experiment.
4. The suppressed decay of $\eta_2(1870)$ into $K^*(892) K$ is the result of a destructive interference due to a large and negative strange-nonstrange mixing angle (similar to the one in the pseudoscalar sector).

In conclusion, it is possible to interpret the resonances [$\pi_2(1670)$, $K_2(1770)$, $\eta_2(1645)$, $\eta_2(1870)$] as the ground-state $\bar{q}q$ pseudotensor mesons nonet if a large and negative mixing angle of about -42° is considered. In this respect, there is – at the stage of the present experimental knowledge – no need to include further additional fields, such as an hybrid pseudotensor state, in the model. (In principle, also a pseudotensor glueball could mix. At the present stage, its mass, as predicted by lattice QCD, is ≈ 3 GeV [17], therefore too large for a sizable effect on decay patterns, see Sec. 5 for predictions of pseudotensor glueball decays). Yet, there are some experimental conflicting results on branching ratios which we discuss in the next subsection.

4.3 Branching ratios of $\eta_2(1870)$

We discuss the branching ratios of the resonance $\eta_2(1870)$. The experimental information is summarized in Tab. (7).

$\eta_2(1870)$			
Branching ratio	Theory	Experiment	Collaboration
$\Gamma^{\text{exp}}(a_2(1320)\pi)/\Gamma^{\text{exp}}(f_2(1270)\eta)$	≈ 23.5	1.7 ± 0.4	average by [1]
		1.60 ± 0.4	Anisovich et al. [32]
		20.4 ± 6.6	Barberis et al. [33]
		4.1 ± 2.3	Adomeit [34]
$\Gamma^{\text{exp}}(a_2(1320)\pi)/\Gamma^{\text{exp}}(a_0(980)\pi)$		32.6 ± 12.6	Barberis et al. [33]
$\Gamma^{\text{exp}}(a_0(980)\pi)/\Gamma^{\text{exp}}(f_2(1270)\eta)$		0.48 ± 0.45	Barberis et al. [33]

Table 7: Theoretical and experimental branching ratios for $\eta_2(1870)$. The mixing angle $\beta_{pt} \approx -42^\circ$ is used for theoretical predictions. Bold numbers are also bold in PDG [1].

Some of the measurements of the branching ratios $\Gamma^{\text{exp}}(a_2(1320)\pi)/\Gamma^{\text{exp}}(f_2(1270)\eta)$ and the average taken by [1] are not in agreement. The value of Barberis et al. (for the WA102 collaboration) is much larger (20.4 ± 6.6) than the others, and was criticized in the recent reanalysis of Anisovich et al. [32]. Actually, the PDG value 1.7 ± 0.4 seems to be solely derived by the result of Anisovich et al. [32] (1.6 ± 0.4), but it is not clear why the central values differ.

It is also instructive to take the product of the bottom two branching ratios from Tab. (7), which should give an estimate for the branching ratio $\Gamma^{\text{exp}}(a_2(1320)\pi)/\Gamma^{\text{exp}}(f_2(1270)\eta)$,

$$\begin{aligned}
 & [\Gamma(a_2(1320)\pi)/\Gamma(f_2(1270)\eta)]^* = \\
 &= [\Gamma^{\text{exp}}(a_2(1320)\pi)/\Gamma^{\text{exp}}(a_0(980)\pi)] \cdot [\Gamma^{\text{exp}}(a_0(980)\pi)/\Gamma^{\text{exp}}(f_2(1270)\eta)] \approx \\
 &\approx (16 \pm 16)^*.
 \end{aligned} \tag{4.3}$$

*(derived from other exp. branchings)

Because of the large errors, this result is in principle compatible with both Anisovich and Barberis, yet the central value is much closer to the latter. New experimental results with a smaller error for the ratio $\Gamma^{\text{exp}}(a_0(980)\pi)/\Gamma^{\text{exp}}(f_2(1270)\eta)$ would be very useful.

Next, we turn to our prediction (obtained by using $\beta_{pt} = -42^\circ$ in our model). We added this result to Tab. (7). For $[\eta_2(1870) \rightarrow a_2(1320)\pi]/[\eta_2(1870) \rightarrow f_2(1270)\eta]$ it reads ≈ 23.5 , hence it strongly supports the branching ratio measured by Barberis [33]. [The bottom two ratios are not directly included in our model, because $a_0(980)$, as well as all scalar mesons, are not part of it. Hence, the corresponding slots in Tab. (7) are empty.]

For better understanding of our prediction (≈ 23.5), it is instructive to have a closer look at the theoretical expression for the branching ratio $\Gamma^{th}(a_2(1320)\pi)/\Gamma^{th}(f_2(1270)\eta)$ of $\eta_2(1870)$. Using Eqs. (2.14) and (A.2) we find,

$$\Gamma^{th}(a_2(1320)\pi)/\Gamma^{th}(f_2(1270)\eta) = \frac{3 \sin^2 \beta_{pt}}{[-\sin \beta_{pt} \cos \beta_t \cos \beta_p + \sqrt{2} \cos \beta_{pt} \sin \beta_t \sin \beta_p]^2} \left[\frac{4 \frac{p_1^5}{m_{a_2}^4} + 30 \frac{p_1^3}{m_{a_2}^2} + 45 p_1}{4 \frac{k_1^5}{m_{f_2}^4} + 30 \frac{k_1^3}{m_{f_2}^2} + 45 k_1} \right], \quad (4.4)$$

where $p_1 = k_f(m_{\eta(1870)}, m_{a_2}, m_\pi)$ and $k_1 = k_f(m_{\eta(1870)}, m_{f_2}, m_\eta)$. Since β_t is very small ($\beta_t = 3.2^\circ$), for $|\beta_{pt}|$ sufficiently large ($\gtrsim 30^\circ$) the first term in Eq. (4.4) can be approximated by $3/\cos^2 \beta_p$, which is independent on β_{pt} . The complete behavior of ratio is plotted as function of β_{pt} in Fig. (2).

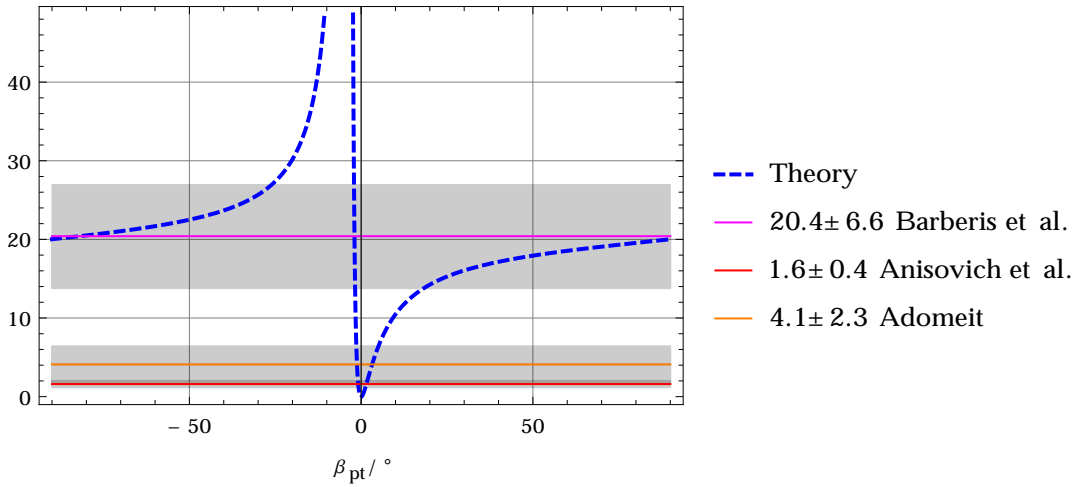


Figure 2: β_{pt} -dependency of the branching ratio $\Gamma(a_2(1320)\pi)/\Gamma(f_2(1270)\eta)$ of $\eta_2(1870)$. The bands correspond to the experimental values, see Tab. (7).

One can see that an agreement with Barberis et al. [33] is reached for a quite broad range of angles (and – most importantly – fits well with $\beta_{pt} \approx -40^\circ$). An agreement with Anisovich et al. [32] is only realized for values very close $\beta_{pt} \approx 0^\circ$, which is however excluded by the other constraints studied in Subsecs. 4.1 and 4.2.

In conclusion of the present discussion, $\eta_2(1645)$ and $\eta_2(1870)$ can be considered as the members of the lowest quark-antiquark nonet only if a large-value (≈ 23) of the branching ratio $\Gamma(a_2(1320)\pi)/\Gamma(f_2(1270)\eta)$ of $\eta_2(1870)$ holds. Within this respect, the result of Anisovich (ratio 1.6 ± 0.4) would point to a different nature of the resonance $\eta_2(1870)$ (see the discussion in Ref. [9]). A new experimental study of the resonance $\eta_2(1870)$ is necessary to understand which is the correct experimental value. In a near future, both experiments GlueX [13–15] and CLAS12 [16] (with more emphasis on the former) can study such mesons via photoproduction, hence shading light on this puzzle of mesonic physics. In general, a new determination by GlueX and CLAS12 of the whole pseudotensor sector would be of great help.

5 Pseudotensor glueball

Glueballs, bound states formed solely by gluons, have not yet been discovered experimentally (for reviews see Refs. [22, 41–49]). While some experimental candidates for low-lying glueballs have been proposed, the situation above 3 GeV is still unsatisfactory. It is then useful to make some (qualitative) predictions of the decay channels of such glueballs in order to help the future experimental identification of candidates.

Among the expected glueballs above 3 GeV, also a glueball with pseudotensor quantum numbers is expected. This (yet hypothetical) state has a lattice-predicted mass of about 3.04 GeV [17, 18] (for general reviews on glueballs, see Refs. [35–37]). The effective Lagrangian(s) describing the decays of this glueball can be obtained by Eqs. (2.6) and (2.7) by recalling that each glueball is flavour-blind (see, for instance, the analogous case of the tensor glueball studied in [5]). The coupling of the glueball to vector-pseudoscalar pairs is expected to be proportional to $G_{\mu\nu} \text{Tr}\{[V^\mu, (\partial^\nu P)]_-\} = 0$, hence vanishes. We then expect that

$$\Gamma_{G \rightarrow VP} = 0 \quad (5.1)$$

for all vector-pseudoscalar channels. This is by itself an important information in the identification of possible candidates. In particular, we predict that $\Gamma_{G \rightarrow \rho\pi} = \Gamma_{G \rightarrow K^*(892)K} = 0$.

The coupling of the glueball to tensor-pseudoscalar pairs is given by

$$\mathcal{L}_{GXP} = c_{GXP} G_{\mu\nu} \text{Tr}(\{X^{\mu\nu}, P\}_+) \neq 0, \quad (5.2)$$

where c_{GXP} denotes is the corresponding coupling constant (with dimension energy). The latter cannot be fixed at present because no information on the full width of this glueball state is available (according to large- N_c it should be smaller than ordinary mesonic states). [The expanded version of the Lagrangian (5.2) is shown in App. A.3.]

We produce an estimate for ratios of decays, which can be easily calculated following the same steps of the previous sections. They are reported in Tab. (8). The glueball mass is assumed to be 3040 MeV sharp.

“ $G_2(3040)$ ”	
Branching ratio	Theory
$\Gamma^{\text{th}}(a_2(1320)\pi)/\Gamma^{\text{th}}(K_2^*(1430)K + c.c.)$	0.9
$\Gamma^{\text{th}}(a_2(1320)\pi)/\Gamma^{\text{th}}(f_2(1270)\eta)$	6.0
$\Gamma^{\text{th}}(a_2(1320)\pi)/\Gamma^{\text{th}}(f_2(1270)\eta'(958))$	8.5
$\Gamma^{\text{th}}(a_2(1320)\pi)/\Gamma^{\text{th}}(f_2'(1525)\eta)$	9.0
$\Gamma^{\text{th}}(a_2(1320)\pi)/\Gamma^{\text{th}}(f_2'(1525)\eta'(958))$	11.0

Table 8: Theoretical branching ratios for the pseudotensor glueball “ $G_2(3040)$ ”.

It is visible that the decays into $K_2^*(1430)K$ and $a_2(1320)\pi$ are the largest (they are enhanced by isospin factors). It must be stressed that the results of Tab. (8) are determined from the single large- N_c and flavour-invariant dominant term of Eq. (5.2) (the constant c_{GXP} scales as N_c^{-1}). In line with the expansions described in Sec. 2.2, further terms proportional $c_{GXP}\delta_s$ as well as $\tilde{c}_{GXP} \propto N_c^{-2}$ and so on, are expected. Similarly, a small but non-vanishing decay’s amplitude of the pseudotensor glueball into a vector-pseudoscalar pair proportional to δ_s also emerges. All these subleading effects will be important when a suitable glueball’s candidate will be experimentally observed.

The search of glueballs between 2.5 – 3 GeV is currently ongoing at BESIII experiment [38, 39] and will be one of the main subjects of the planned PANDA experiment at the FAIR facility in Darmstadt [40]. In particular, at PANDA the pseudotensor glueball can be directly formed by proton-antiproton fusion, hence it can be investigated in detail. The here discussed theoretical branching ratios provide help toward the identification of possible candidates by looking at their decay patterns. The full decay width cannot be obtained, however according to large- N_c [24–26] it should be smaller than conventional quark-antiquark states. A value of about few MeV (≈ 10 MeV) seems to be a rational guess, see the discussion in Ref. [21].

6 Discussions and conclusions

In this work we have studied the phenomenology of the ground-state $\bar{q}q$ pseudotensor meson nonet, identified with the resonances $[\pi_2(1670), K_2(1770), \eta_2(1645), \eta_2(1870)]$, by using a quantum field theoretical approach. Two effective interaction Lagrangians which couple pseudotensor states to pseudoscalar, vector and tensor ones were constructed and used to study decays and mixing.

The resonances $\pi_2(1670)$ and $K_2(1770)$ fit very well into the $\bar{q}q$ picture. However, the isoscalar states $\eta_2(1645), \eta_2(1870)$ are more subtle. A small mixing angle between purely nonstrange and strange state is at odd with the experimental data [$\eta_2(1645) \rightarrow a_2(1320)\pi$ is larger than 300 MeV and overshoots the total experimental width]. A detailed study of the isoscalar sector shows that a good agreement with data is possible if the strange-nonstrange mixing angle is large and negative [approximately -42° , see Fig. (1)].

There is however an issue that still needs to be clarified: the ratio $[\eta_2(1870) \rightarrow a_2(1320)\pi]/[\eta_2(1870) \rightarrow f_2(1270)\eta]$ reads 20.4 ± 6.6 by Barberis [33] and 1.6 ± 0.4 by Anisovich [32]. PDG [1] lately opted for the latter result (1.7 ± 0.4 , with a slightly modified central value). Our study shows that a quarkonium interpretation of $\eta_2(1870)$ implies a ratio of about ≈ 23 , hence in good agreement with Barberis but in disagreement with Anisovich. In this respect, a future experimental clarification of this issue is compelling. There are mainly two possible outcomes:

- a) The ratio quoted by Barberis turns out to be correct, then we have good candidates for a ground-state pseudoscalar meson nonet. However, the large mixing angle (comparable to the one in the pseudoscalar sector) would be a mystery which will deserve a more profound study. Namely, besides the pseudoscalar sector which is affected by the chiral anomaly, all strange-nonstrange mixing angles are small (vector, axial-vector, tensor sectors [1, 3, 5, 7]). Where would such a large mixing in the pseudotensor sector come from? Would the two-gluon exchange diagram be also enhanced in the pseudotensor channel (a side-effect of the chiral anomaly)?
- b) If, on the contrary, the result of Anisovich shall be confirmed, an understanding of the low-lying pseudotensor states as a standard quark-antiquark nonet would be hard. Modifications would be needed. For instance, one could include additional states in the current approach (such as an hybrid pseudotensor state) which can mix with ordinary $\bar{q}q$ states and change their decay ratios. In such a scenario one would need to consider a decuplet of states (9 standard quarkonia and one additional hybrid state, similar to the decuplet study of scalar states between 1.3 – 1.8 GeV [22, 41–46]). We leave such an analysis for the future, if there will be compelling evidence that the easiest scenario with a low-lying $\bar{q}q$ nonet fails (this is not yet the case, as we have discussed in this work).

As a byproduct of our study, we have also studied the decays of a putative pseudotensor glueball state with a mass of 3.04 GeV. We find that at leading order it does not decay into pseudoscalar-vector meson pairs (such as $\rho(770)\pi$ and $K^*(892)K + c.c.$). On the contrary, sizable decays into $K_2^*(1430)K + c.c.$ and $a_2(1320)\pi$ are expected.

Further improvements of our model (besides the enlargement to a decuplet of states mentioned above) is the inclusion of large- N_c suppressed terms and terms breaking flavor symmetry. Moreover, tensor and pseudotensor mesons can also build a chiral multiplet. They could be then coupled to the extended Linear Sigma Model in order to test chiral symmetry (and its spontaneous breaking) in the (pseudo)tensor sector. Also the study of (pseudo)tensor glueballs can be extended in this way. As shown in Ref. [21, 47–49], chiral symmetry imposes further constraints on the decays of glueballs, hence improving the predictive powers of hadronic models. From the experimental side, new results and determinations of the pseudotensor mesons $[\pi_2(1670), K_2(1770), \eta_2(1645), \eta_2(1870)]$ are needed to test the standard basic quark-anti-quark scenario and the existence or not of an enhanced mixing in the isoscalar sector. The upcoming experiments GlueX and CLAS12 experiments at Jlab are expected to provide results in this direction. Indeed, the properties of pseudotensor mesons are also investigated in the light-meson program of the COMPASS experiment [50].

Acknowledgments: The authors thank Dirk H. Rischke for useful discussions. F.G. acknowledges support from the Polish National Science Centre (NCN) through the OPUS project nr. 2015/17/B/ST2/01625. A.K. thanks Dennis D. Dietrich for instructive discussions.

The final publication is available at Springer via <http://dx.doi.org/10.1140/epja/i2016-16356-x>.

A Extended form of the Lagrangians of the model

The explicit expression for the interaction Lagrangian (2.6) coupling pseudotensor mesons to vector and pseudoscalar ones is given by:

$$\begin{aligned}
\mathcal{L}_{TVP} &= c_{TVP} \text{Tr}\{T_{\mu\nu}[V^\mu, (\partial^\nu P)]_-\} = \tag{A.1} \\
&= c_{TVP} \left(\frac{1}{\sqrt{2}} \pi_{2,\mu\nu}^0 \left[\bar{K}^{*0\mu}(\partial^\nu K^0) - K^{*0\mu}(\partial^\nu \bar{K}^0) + K^{*+\mu}(\partial^\nu K^-) - K^{*-\mu}(\partial^\nu K^+) + \right. \right. \\
&\quad \left. \left. + 2\rho^{+\mu}(\partial^\nu \pi^-) - 2\rho^{-\mu}(\partial^\nu \pi^+) \right] + \right. \\
&\quad + \pi_{2,\mu\nu}^+ \left[K^{*0\mu}(\partial^\nu K^-) - K^{*-\mu}(\partial^\nu K^0) + \sqrt{2}\rho^{-\mu}(\partial^\nu \pi^0) - \sqrt{2}\rho^{0\mu}(\partial^\nu \pi^-) \right] + \\
&\quad + \pi_{2,\mu\nu}^- \left[K^{*+\mu}(\partial^\nu \bar{K}^0) - \bar{K}^{*0\mu}(\partial^\nu K^+) + \sqrt{2}\rho^{0\mu}(\partial^\nu \pi^+) - \sqrt{2}\rho^{+\mu}(\partial^\nu \pi^0) \right] + \\
&\quad + K_{2,\mu\nu}^0 \left\{ -\frac{1}{\sqrt{2}} \bar{K}^{*0\mu}(\partial^\nu \pi^0) + K^{*-\mu}(\partial^\nu \pi^+) + \frac{1}{\sqrt{2}} \rho^{0\mu}(\partial^\nu \bar{K}^0) - \rho^{+\mu}(\partial^\nu K^-) + \right. \\
&\quad \left. + \frac{1}{\sqrt{2}} \bar{K}^{*0\mu} [(\partial^\nu \eta)(\cos \beta_p - \sqrt{2} \sin \beta_p) + (\partial^\nu \eta')(-\sin \beta_p - \sqrt{2} \cos \beta_p)] + \right. \\
&\quad \left. + \frac{1}{\sqrt{2}} [\omega^\mu(-\cos \beta_v + \sqrt{2} \sin \beta_v) + \phi^\mu(\sin \beta_v + \sqrt{2} \cos \beta_v)](\partial^\nu \bar{K}^0) \right\} + \\
&\quad + K_{2,\mu\nu}^+ \left\{ \frac{1}{\sqrt{2}} K^{*-\mu}(\partial^\nu \pi^0) + \bar{K}^{*0\mu}(\partial^\nu \pi^-) - \frac{1}{\sqrt{2}} \rho^{0\mu}(\partial^\nu K^-) - \rho^{-\mu}(\partial^\nu \bar{K}^0) + \right. \\
&\quad \left. + \frac{1}{\sqrt{2}} K^{*-\mu} [(\partial^\nu \eta)(\cos \beta_p - \sqrt{2} \sin \beta_p) + (\partial^\nu \eta')(-\sin \beta_p - \sqrt{2} \cos \beta_p)] + \right. \\
&\quad \left. + \frac{1}{\sqrt{2}} [\omega^\mu(-\cos \beta_v + \sqrt{2} \sin \beta_v) + \phi^\mu(\sin \beta_v + \sqrt{2} \cos \beta_v)](\partial^\nu K^-) \right\} + \\
&\quad + K_{2,\mu\nu}^- \left\{ -\frac{1}{\sqrt{2}} K^{*+\mu}(\partial^\nu \pi^0) - K^{*0\mu}(\partial^\nu \pi^+) + \frac{1}{\sqrt{2}} \rho^{0\mu}(\partial^\nu K^+) + \rho^{+\mu}(\partial^\nu K^0) + \right. \\
&\quad \left. + \frac{1}{\sqrt{2}} K^{*+\mu} [(\partial^\nu \eta)(-\cos \beta_p + \sqrt{2} \sin \beta_p) + (\partial^\nu \eta')(\sin \beta_p + \sqrt{2} \cos \beta_p)] + \right. \\
&\quad \left. + \frac{1}{\sqrt{2}} [\omega^\mu(\cos \beta_v - \sqrt{2} \sin \beta_v) + \phi^\mu(-\sin \beta_v - \sqrt{2} \cos \beta_v)](\partial^\nu K^+) \right\} + \\
&\quad + \bar{K}_{2,\mu\nu}^0 \left\{ \frac{1}{\sqrt{2}} K^{*0\mu}(\partial^\nu \pi^0) - K^{*+\mu}(\partial^\nu \pi^-) - \frac{1}{\sqrt{2}} \rho^{0\mu}(\partial^\nu K^0) + \rho^{-\mu}(\partial^\nu K^+) + \right. \\
&\quad \left. + \frac{1}{\sqrt{2}} K^{*0\mu} [(\partial^\nu \eta)(-\cos \beta_p + \sqrt{2} \sin \beta_p) + (\partial^\nu \eta')(\sin \beta_p + \sqrt{2} \cos \beta_p)] + \right. \\
&\quad \left. + \frac{1}{\sqrt{2}} [\omega^\mu(\cos \beta_v - \sqrt{2} \sin \beta_v) + \phi^\mu(-\sin \beta_v - \sqrt{2} \cos \beta_v)](\partial^\nu K^0) \right\} + \\
&\quad + \frac{1}{\sqrt{2}} \eta_{2,\mu\nu} (-\cos \beta_{pt} + \sqrt{2} \sin \beta_{pt}) \cdot \\
&\quad \cdot [\bar{K}^{*0\mu}(\partial^\nu K^0) - K^{*0\mu}(\partial^\nu \bar{K}^0) - K^{*+\mu}(\partial^\nu K^-) + K^{*-\mu}(\partial^\nu K^+)] +
\end{aligned}$$

$$\begin{aligned}
& + \frac{1}{\sqrt{2}} \eta'_{2,\mu\nu} (\sin \beta_{pt} + \sqrt{2} \cos \beta_{pt}) \cdot \\
& \cdot [\bar{K}^{*0\mu} (\partial^\nu K^0) - K^{*0\mu} (\partial^\nu \bar{K}^0) - K^{*+\mu} (\partial^\nu K^-) + K^{*-\mu} (\partial^\nu K^+)] \Big).
\end{aligned}$$

Similarly, the explicit expression of Eq. (2.7) reads:

$$\begin{aligned}
\mathcal{L}_{TXP} &= c_{TXP} \text{Tr}(T_{\mu\nu} \{X^{\mu\nu}, P\}_+) = \tag{A.2} \\
&= c_{TXP} \left(\frac{1}{\sqrt{2}} \pi_{2,\mu\nu}^0 (-\bar{K}_2^{*0\mu\nu} K^0 - K_2^{*0\mu\nu} \bar{K}^0 + K_2^{*+\mu\nu} K^- + K_2^{*-\mu\nu} K^+ + \right. \\
&\quad + 2 f_2^{\mu\nu} \cos \beta_t \pi^0 - 2 f_2^{\prime\mu\nu} \sin \beta_t \pi^0 + 2 a_2^{0\mu\nu} \eta \cos \beta_p - 2 a_2^{0\mu\nu} \eta' \sin \beta_p) + \\
&\quad + \pi_{2,\mu\nu}^+ (K_2^{*0\mu\nu} K^- + K_2^{*-\mu\nu} K^0 + \sqrt{2} f_2^{\mu\nu} \cos \beta_t \pi^- - \sqrt{2} f_2^{\prime\mu\nu} \sin \beta_t \pi^- + \\
&\quad + \sqrt{2} a_2^{-\mu\nu} \eta \cos \beta_p - \sqrt{2} a_2^{-\mu\nu} \eta' \sin \beta_p) + \\
&\quad + \pi_{2,\mu\nu}^- (\bar{K}_2^{*0\mu\nu} K^+ + K_2^{*+\mu\nu} \bar{K}^0 + \sqrt{2} f_2^{\mu\nu} \cos \beta_t \pi^+ - \sqrt{2} f_2^{\prime\mu\nu} \sin \beta_t \pi^+ + \\
&\quad + \sqrt{2} a_2^{+\mu\nu} \eta \cos \beta_p - \sqrt{2} a_2^{+\mu\nu} \eta' \sin \beta_p) + \\
&\quad + K_{2,\mu\nu}^0 \left\{ -\frac{1}{\sqrt{2}} \bar{K}_2^{*0\mu\nu} \pi^0 + K_2^{*-\mu\nu} \pi^+ - \frac{1}{\sqrt{2}} a_2^{0\mu\nu} \bar{K}^0 + a_2^{+\mu\nu} K^- + \right. \\
&\quad + \frac{1}{\sqrt{2}} \bar{K}_2^{*0\mu\nu} [\eta (\cos \beta_p + \sqrt{2} \sin \beta_p) + \eta' (-\sin \beta_p + \sqrt{2} \cos \beta_p)] + \\
&\quad + \frac{1}{\sqrt{2}} [f_2^{\mu\nu} (\cos \beta_t + \sqrt{2} \sin \beta_t) + f_2^{\prime\mu\nu} (-\sin \beta_t + \sqrt{2} \cos \beta_t)] \bar{K}^0 \Big\} + \\
&\quad + K_{2,\mu\nu}^+ \left\{ \frac{1}{\sqrt{2}} K_2^{*-\mu\nu} \pi^0 + \bar{K}_2^{*0\mu\nu} \pi^- + \frac{1}{\sqrt{2}} a_2^{0\mu\nu} K^- + a_2^{-\mu\nu} \bar{K}^0 + \right. \\
&\quad + \frac{1}{\sqrt{2}} K_2^{*-\mu\nu} [\eta (\cos \beta_p + \sqrt{2} \sin \beta_p) + \eta' (-\sin \beta_p + \sqrt{2} \cos \beta_p)] + \\
&\quad + \frac{1}{\sqrt{2}} [f_2^{\mu\nu} (\cos \beta_t + \sqrt{2} \sin \beta_t) + f_2^{\prime\mu\nu} (-\sin \beta_t + \sqrt{2} \cos \beta_t)] K^- \Big\} + \\
&\quad + K_{2,\mu\nu}^- \left\{ \frac{1}{\sqrt{2}} K_2^{*+\mu\nu} \pi^0 + K_2^{*0\mu\nu} \pi^+ + \frac{1}{\sqrt{2}} a_2^{0\mu\nu} K^+ + a_2^{+\mu\nu} K^0 + \right. \\
&\quad + \frac{1}{\sqrt{2}} K_2^{*+\mu\nu} [\eta (\cos \beta_p + \sqrt{2} \sin \beta_p) + \eta' (-\sin \beta_p + \sqrt{2} \cos \beta_p)] + \\
&\quad + \frac{1}{\sqrt{2}} [f_2^{\mu\nu} (\cos \beta_t + \sqrt{2} \sin \beta_t) + f_2^{\prime\mu\nu} (-\sin \beta_t + \sqrt{2} \cos \beta_t)] K^+ \Big\} + \\
&\quad + \bar{K}_{2,\mu\nu}^0 \left\{ -\frac{1}{\sqrt{2}} K_2^{*0\mu\nu} \pi^0 + K_2^{*+\mu\nu} \pi^- - \frac{1}{\sqrt{2}} a_2^{0\mu\nu} K^0 + a_2^{-\mu\nu} K^+ + \right. \\
&\quad + \frac{1}{\sqrt{2}} K_2^{*0\mu\nu} [\eta (\cos \beta_p + \sqrt{2} \sin \beta_p) + \eta' (-\sin \beta_p + \sqrt{2} \cos \beta_p)] + \\
&\quad + \frac{1}{\sqrt{2}} [f_2^{\mu\nu} (\cos \beta_t + \sqrt{2} \sin \beta_t) + f_2^{\prime\mu\nu} (-\sin \beta_t + \sqrt{2} \cos \beta_t)] K^0 \Big\} + \\
&\quad + \frac{1}{\sqrt{2}} \eta_{2,\mu\nu} [(\cos \beta_{pt} + \sqrt{2} \sin \beta_{pt}) \cdot \\
&\quad \cdot (\bar{K}_2^{*0\mu\nu} K^0 + K_2^{*0\mu\nu} \bar{K}^0 + K_2^{*+\mu\nu} K^- + K_2^{*-\mu\nu} K^+) +
\end{aligned}$$

$$\begin{aligned}
& + 2 \cos \beta_{pt} (a_2^{0\mu\nu} \pi^0 + a_2^{+\mu\nu} \pi^- + a_2^{-\mu\nu} \pi^+) + \\
& + 2 \cos \beta_{pt} (f_2^{\mu\nu} \cos \beta_t - f_2'^{\mu\nu} \sin \beta_t)(\eta \cos \beta_p - \eta' \sin \beta_p) + \\
& + 2\sqrt{2} \sin \beta_{pt} (f_2^{\mu\nu} \sin \beta_t + f_2'^{\mu\nu} \cos \beta_t)(\eta \sin \beta_p + \eta' \cos \beta_p) \Big] + \\
& + \frac{1}{\sqrt{2}} \eta'_{2,\mu\nu} [(-\sin \beta_{pt} + \sqrt{2} \cos \beta_{pt}) \cdot \\
& \cdot (\bar{K}_2^{*0\mu\nu} K^0 + K_2^{*0\mu\nu} \bar{K}^0 + K_2^{*+\mu\nu} K^- + K_2^{*- \mu\nu} K^+) + \\
& - 2 \sin \beta_{pt} (a_2^{0\mu\nu} \pi^0 + a_2^{+\mu\nu} \pi^- + a_2^{-\mu\nu} \pi^+) + \\
& - 2 \sin \beta_{pt} (f_2^{\mu\nu} \cos \beta_t - f_2'^{\mu\nu} \sin \beta_t)(\eta \cos \beta_p - \eta' \sin \beta_p) + \\
& + 2\sqrt{2} \cos \beta_{pt} (f_2^{\mu\nu} \sin \beta_t + f_2'^{\mu\nu} \cos \beta_t)(\eta \sin \beta_p + \eta' \cos \beta_p) \Big].
\end{aligned}$$

The explicit form of the glueball interaction Lagrangian (5.2) that couples the pseudotensor glueball to tensor and pseudoscalar mesons reads,

$$\begin{aligned}
\mathcal{L}_{GXP} &= c_{GXP} G_{\mu\nu} \text{Tr}(\{X^{\mu\nu}, P\}_+) = \\
&= 2 c_{GXP} G_{\mu\nu} [a_2^{0\mu\nu} \pi^0 + a_2^{+\mu\nu} \pi^- + a_2^{-\mu\nu} \pi^+ + \\
&\quad + \bar{K}_2^{*0\mu\nu} K^0 + K_2^{*0\mu\nu} \bar{K}^0 + K_2^{*+\mu\nu} K^- + K_2^{*- \mu\nu} K^+ + \\
&\quad + (f_2^{\mu\nu} \cos \beta_t - f_2'^{\mu\nu} \sin \beta_t)(\eta \cos \beta_p - \eta' \sin \beta_p) + \\
&\quad + (f_2^{\mu\nu} \sin \beta_t + f_2'^{\mu\nu} \cos \beta_t)(\eta \sin \beta_p + \eta' \cos \beta_p) \Big].
\end{aligned} \tag{A.3}$$

B Unpolarized invariant decay amplitudes

In this appendix we calculate the unpolarized invariant decay amplitudes $\frac{1}{5} \sum |\mathcal{M}|^2$ for the decay widths (2.13) and (2.14). We use Feynman rules to translate the Lagrangian densities (2.6) and (2.7) into decay amplitudes. Therefore, the trace and matrix structures of the given Lagrangians only modify the specific coupling constants of the single decay channels. Consequently, we work with the simplified Lagrangian densities

$$\mathcal{L}_{TVP} = g_{TVP} T_{\mu\nu} V^\mu (\partial^\nu P), \tag{B.1}$$

$$\mathcal{L}_{TXP} = g_{TXP} T_{\mu\nu} X^{\mu\nu} P. \tag{B.2}$$

The Feynman rules are:

$$\begin{aligned}
g &\rightarrow -i g, \\
T^{\mu\nu} &\rightarrow \epsilon^{\mu\nu}(\lambda_t, \vec{k}_t), \\
X^{\mu\nu} &\rightarrow \epsilon^{\mu\nu}(\lambda_x, \vec{k}_x), \\
V^\mu &\rightarrow \epsilon^\mu(\lambda_v, \vec{k}_v), \\
\partial^\mu &\rightarrow i k_p^\mu,
\end{aligned} \tag{B.3}$$

where $\epsilon^{\mu(\nu)}$ are polarization vectors (tensors), λ is the specific polarizations¹, k^μ is the four-momentum, and \vec{k} is the three-momentum. Hence,

$$i\mathcal{M}_{TVP} = -i g_{TVP} \epsilon_{\mu\nu}(\lambda_t, \vec{k}_t) \epsilon^\mu(\lambda_v, \vec{k}_v) i k_p^\nu = g_{tvp} \epsilon_{\mu\nu}(\lambda_t, \vec{k}_t) \epsilon^\mu(\lambda_v, \vec{k}_v) k_p^\nu, \quad (\text{B.4})$$

$$i\mathcal{M}_{TXP} = -i g_{TXP} \epsilon_{\mu\nu}(\lambda_t, \vec{k}_t) \epsilon^{\mu\nu}(\lambda_x, \vec{k}_x). \quad (\text{B.5})$$

The unpolarized invariant decay amplitudes is found by taking the square of the above expressions. In addition one has to average over all incoming spin-polarizations and sum up all possible outgoing polarizations. For the decay of pseudotensor resonances into a vector and a pseudoscalar mesons we find:

$$\begin{aligned} \frac{1}{5} \sum |\mathcal{M}_{TVP}|^2 &= \frac{g_{TVP}^2}{5} \sum_{\lambda_t=1}^5 \sum_{\lambda_v=1}^3 \epsilon_{\mu\nu}(\lambda_t, \vec{k}_t) \epsilon_{\alpha\beta}(\lambda_t, \vec{k}_t) \epsilon^\mu(\lambda_v, \vec{k}_v) \epsilon^\alpha(\lambda_v, \vec{k}_v) k_p^\nu k_p^\beta = \\ &= \frac{g_{tvp}^2}{15} \left(2 \frac{|\vec{k}|^4}{m_v^2} + 5 |\vec{k}|^2 \right), \end{aligned} \quad (\text{B.6})$$

where the rest frame of the decaying pseudo-tensor meson is considered (\vec{k} denotes the momentum of an outgoing particle: $|\vec{k}| = k_f(m_T, m_V, m_P)$). We made use of the following completeness relations

$$\sum_{\lambda=1}^3 \epsilon_\mu(\lambda, \vec{k}) \epsilon_\nu(\lambda, \vec{k}) = -G_{\mu\nu}, \quad (\text{B.7})$$

$$\sum_{\lambda=1}^5 \epsilon_{\mu\nu}(\lambda, \vec{k}) \epsilon_{\alpha\beta}(\lambda, \vec{k}) = -\frac{G_{\mu\nu} G_{\alpha\beta}}{3} + \frac{G_{\mu\alpha} G_{\nu\beta} + G_{\mu\beta} G_{\nu\alpha}}{2}, \quad (\text{B.8})$$

where

$$G_{\mu\nu} = \eta_{\mu\nu} - \frac{k_\mu k_\nu}{m^2}. \quad (\text{B.9})$$

(For details, see Ref. [19] and refs. therein). In analogy to the previous case, the unpolarized invariant decay amplitude for the decay of pseudotensor meson into a tensor and a pseudoscalar mesons reads:

$$\begin{aligned} \frac{1}{5} \sum |\mathcal{M}_{TXP}|^2 &= \frac{g_{TXP}^2}{5} \sum_{\lambda_t=1}^5 \sum_{\lambda_x=1}^5 \epsilon_{\mu\nu}(\lambda_t, \vec{k}_t) \epsilon_{\alpha\beta}(\lambda_t, \vec{k}_t) \epsilon^{\mu\nu}(\lambda_x, \vec{k}_x) \epsilon^{\alpha\beta}(\lambda_x, \vec{k}_x) = \\ &= \frac{g_{TXP}^2}{45} \left(4 \frac{|\vec{k}|^4}{m_X^4} + 30 \frac{|\vec{k}|^2}{m_X^2} + 45 \right) \end{aligned} \quad (\text{B.10})$$

where $|\vec{k}| = k_f(m_T, m_X, m_P)$.

References

- [1] K. A. Olive *et al.* [Particle Data Group Collaboration], “Review of Particle Physics,” *Chin. Phys. C* **38** (2014) 090001. doi:10.1088/1674-1137/38/9/090001.

¹For tensors $\lambda = -2, -1, 0, +1, +2$, whereas for vectors $\lambda = -1, 0, +1$, representing the spin projections, or respective degrees of freedom.

- [2] S. Godfrey and N. Isgur, “Mesons in a Relativized Quark Model with Chromodynamics,” *Phys. Rev. D* **32** (1985) 189. doi:10.1103/PhysRevD.32.189.
- [3] E. Klempt and A. Zaitsev, “Glueballs, Hybrids, Multiquarks. Experimental facts versus QCD inspired concepts,” *Phys. Rept.* **454** (2007) 1 doi:10.1016/j.physrep.2007.07.006 [arXiv:0708.4016 [hep-ph]].
- [4] D. Parganlija, P. Kovacs, G. Wolf, F. Giacosa and D. H. Rischke, “Meson vacuum phenomenology in a three-flavor linear sigma model with (axial-)vector mesons,” *Phys. Rev. D* **87** (2013) no.1, 014011 doi:10.1103/PhysRevD.87.014011 [arXiv:1208.0585 [hep-ph]].
- [5] F. Giacosa, T. Gutsche, V. E. Lyubovitskij and A. Faessler, “Decays of tensor mesons and the tensor glueball in an effective field approach,” *Phys. Rev. D* **72** (2005) 114021 doi:10.1103/PhysRevD.72.114021 [hep-ph/0511171].
- [6] L. Burakovsky and J. T. Goldman, “Towards resolution of the enigmas of P wave meson spectroscopy,” *Phys. Rev. D* **57** (1998) 2879 doi:10.1103/PhysRevD.57.2879 [hep-ph/9703271].
- [7] V. Cirigliano, G. Ecker, H. Neufeld and A. Pich, “Meson resonances, large $N(c)$ and chiral symmetry,” *JHEP* **0306** (2003) 012 doi:10.1088/1126-6708/2003/06/012 [hep-ph/0305311].
- [8] B. Wang, C. Q. Pang, X. Liu and T. Matsuki, “Pseudotensor meson family,” *Phys. Rev. D* **91** (2015) no.1, 014025 doi:10.1103/PhysRevD.91.014025 [arXiv:1410.3930 [hep-ph]].
- [9] C. Bing, K. W. Wei and A. Zhang, “ $X(1870)$ and $\eta_2(1870)$: Which can be assigned as a hybrid state?,” *Adv. High Energy Phys.* **2013** (2013) 217858 doi:10.1155/2013/217858 [arXiv:1304.6190 [hep-ph]].
- [10] G. Amelino-Camelia *et al.*, “Physics with the KLOE-2 experiment at the upgraded DAΦNE,” *Eur. Phys. J. C* **68** (2010) 619 doi:10.1140/epjc/s10052-010-1351-1 [arXiv:1003.3868 [hep-ex]].
- [11] T. Feldmann, P. Kroll and B. Stech, “Mixing and decay constants of pseudoscalar mesons,” *Phys. Rev. D* **58** (1998) 114006 doi:10.1103/PhysRevD.58.114006 [hep-ph/9802409].
- [12] G. 't Hooft, “How Instantons Solve the $U(1)$ Problem,” *Phys. Rept.* **142** (1986) 357. doi:10.1016/0370-1573(86)90117-1.
- [13] H. Al Ghouli *et al.* [GlueX Collaboration], “First Results from The GlueX Experiment,” *AIP Conf. Proc.* **1735** (2016) 020001 doi:10.1063/1.4949369 [arXiv:1512.03699 [nucl-ex]].
- [14] B. Zihlmann [GlueX Collaboration], “GlueX a new facility to search for gluonic degrees of freedom in mesons,” *AIP Conf. Proc.* **1257** (2010) 116. doi:10.1063/1.3483306.
- [15] M. Shepherd, “GlueX at Jefferson Lab: a search for exotic states of matter in photon-proton collisions,” *PoS Bormio* **2014** (2014) 004.
- [16] A. Rizzo [CLAS Collaboration], “The meson spectroscopy program with CLAS12 at Jefferson Laboratory,” *PoS CD* **15** (2016) 060.
- [17] Y. Chen *et al.*, “Glueball spectrum and matrix elements on anisotropic lattices,” *Phys. Rev. D* **73** (2006) 014516 doi:10.1103/PhysRevD.73.014516 [hep-lat/0510074].
- [18] E. Gregory, A. Irving, B. Lucini, C. McNeile, A. Rago, C. Richards and E. Rinaldi, “Towards the glueball spectrum from unquenched lattice QCD,” *JHEP* **1210**, 170 (2012) doi:10.1007/JHEP10(2012)170 [arXiv:1208.1858[hep-lat]].
- [19] A. Koenigstein, F. Giacosa and D. H. Rischke, “Classical and quantum theory of the massive spin-two field,” *Annals Phys.* **368** (2016) 16 doi:10.1016/j.aop.2016.01.024, [arXiv:1508.00110 [hep-th]].

- [20] F. Divotgey, L. Olbrich and F. Giacosa, “Phenomenology of axial-vector and pseudovector mesons: decays and mixing in the kaonic sector,” *Eur. Phys. J. A* **49** (2013) 135 doi:10.1140/epja/i2013-13135-3 [arXiv:1306.1193 [hep-ph]].
- [21] F. Giacosa, J. Sammet and S. Janowski, “Decays of the vector glueball,” arXiv:1607.03640 [hep-ph].
- [22] C. Amsler and F. E. Close, “Is $f_0(1500)$ a scalar glueball?,” *Phys. Rev. D* **53** (1996) 295 doi:10.1103/PhysRevD.53.295 [hep-ph/9507326].
- [23] F. Giacosa, T. Gutsche and A. Faessler, “A Covariant constituent quark / gluon model for the glueball-quarkonia content of scalar - isoscalar mesons,” *Phys. Rev. C* **71** (2005) 025202 doi:10.1103/PhysRevC.71.025202 [hep-ph/0408085].
- [24] G. 't Hooft, “A Planar Diagram Theory for Strong Interactions,” *Nucl. Phys. B* **72** (1974) 461. doi:10.1016/0550-3213(74)90154-0.
- [25] E. Witten, “Baryons in the $1/n$ Expansion,” *Nucl. Phys. B* **160** (1979) 57. doi:10.1016/0550-3213(79)90232-3.
- [26] R. F. Lebed, “Phenomenology of large $N(c)$ QCD,” *Czech. J. Phys.* **49** (1999) 1273 doi:10.1023/A:1022820227262 [nucl-th/9810080].
- [27] F. Giacosa and G. Pagliara, “On the spectral functions of scalar mesons,” *Phys. Rev. C* **76** (2007) 065204 doi:10.1103/PhysRevC.76.065204 [arXiv:0707.3594 [hep-ph]].
- [28] S. U. Chung *et al.*, “Exotic and q anti-q resonances in the π^+ π^- π^- system produced in π^- p collisions at 18-GeV/c/,” *Phys. Rev. D* **65** (2002) 072001. doi:10.1103/PhysRevD.65.072001
- [29] D. Barberis *et al.* [WA102 Collaboration], “A Study of the centrally produced π^+ π^- π^0 channel in p p interactions at 450-GeV/c,” *Phys. Lett. B* **422** (1998) 399 doi:10.1016/S0370-2693(98)00063-X [hep-ex/9801003].
- [30] T. A. Armstrong *et al.* [Aachen-Bari-Bonn-CERN-Glasgow-Liverpool-Milan Collaboration], “A Partial Wave Analysis of the $(K^+ K^- \pi^-)$ System Produced in $\pi^- p \rightarrow K^+ K^- \pi^- p$ at 16-GeV/c,” *Nucl. Phys. B* **202** (1982) 1. doi:10.1016/0550-3213(82)90218-8
- [31] J. Kuhn *et al.* [E852 Collaboration], “Exotic meson production in the $f_1(1285)$ π^- system observed in the reaction $\pi^- p \rightarrow \eta \pi^+ \pi^- \pi^- p$ at 18-GeV/c,” *Phys. Lett. B* **595** (2004) 109 doi:10.1016/j.physletb.2004.05.032 [hep-ex/0401004].
- [32] A. V. Anisovich, C. J. Batty, D. V. Bugg, V. A. Nikonov and A. V. Sarantsev, “A fresh look at $\eta_2(1645)$, $\eta_2(1870)$, $\eta_2(2030)$ and $f_2(1910)$ in $\bar{p}p \rightarrow \eta 3\pi^0$,” *Eur. Phys. J. C* **71** (2011) 1511 doi:10.1140/epjc/s10052-010-1511-3 [arXiv:1009.1781 [hep-ex]].
- [33] D. Barberis *et al.* [WA102 Collaboration], “A Spin analysis of the 4 π channels produced in central p p interactions at 450-GeV/c,” *Phys. Lett. B* **471** (2000) 440 doi:10.1016/S0370-2693(99)01413-6 [hep-ex/9912005].
- [34] J. Adomeit *et al.* [Crystal Barrel Collaboration], “Evidence for two isospin zero $J(PC) = 2^-+$ mesons at 1645-MeV and 1875-MeV,” *Z. Phys. C* **71** (1996) 227. doi:10.1007/s002880050166.
- [35] W. Ochs, “The Status of Glueballs,” *J. Phys. G* **40** (2013) 043001 doi:10.1088/0954-3899/40/4/043001 [arXiv:1301.5183 [hep-ph]].
- [36] V. Mathieu, N. Kochelev and V. Vento, “The Physics of Glueballs,” *Int. J. Mod. Phys. E* **18** (2009) 1 doi:10.1142/S0218301309012124 [arXiv:0810.4453 [hep-ph]].
- [37] V. Crede and C. A. Meyer, “The Experimental Status of Glueballs,” *Prog. Part. Nucl. Phys.* **63** (2009) 74 doi:10.1016/j.pnpnp.2009.03.001 [arXiv:0812.0600 [hep-ex]].

- [38] G. Mezzadri, “Light hadron spectroscopy at BESIII,” PoS EPS **-HEP2015** (2015) 423.
- [39] S. Marcello [BESIII Collaboration], “Hadron Physics from BESIII,” JPS Conf. Proc. **10** (2016) 010009. doi:10.7566/JPSCP.10.010009.
- [40] M. F. M. Lutz *et al.* [PANDA Collaboration], “Physics Performance Report for PANDA: Strong Interaction Studies with Antiprotons,” arXiv:0903.3905 [hep-ex].
- [41] C. Amsler and F. E. Close, “Evidence for a scalar glueball,” Phys. Lett. B **353** (1995) 385 doi:10.1016/0370-2693(95)00579-A [hep-ph/9505219].
- [42] M. Strohmeier-Presicek, T. Gutsche, R. Vinh Mau and A. Faessler, “Glueball quarkonia content and decay of scalar - isoscalar mesons,” Phys. Rev. D **60** (1999) 054010 doi:10.1103/PhysRevD.60.054010 [hep-ph/9904461].
- [43] W. J. Lee and D. Weingarten, “Scalar quarkonium masses and mixing with the lightest scalar glueball,” Phys. Rev. D **61** (2000) 014015 doi:10.1103/PhysRevD.61.014015 [hep-lat/9910008].
- [44] F. Giacosa, T. Gutsche, V. E. Lyubovitskij and A. Faessler, “Scalar nonet quarkonia and the scalar glueball: Mixing and decays in an effective chiral approach,” Phys. Rev. D **72** (2005) 094006 doi:10.1103/PhysRevD.72.094006 [hep-ph/0509247].
- [45] H. Y. Cheng, C. K. Chua and K. F. Liu, “Scalar glueball, scalar quarkonia, and their mixing,” Phys. Rev. D **74** (2006) 094005 doi:10.1103/PhysRevD.74.094005 [hep-ph/0607206].
- [46] T. Gutsche, S. Kuleshov, V. E. Lyubovitskij and I. T. Obukhovskiy, “Search for the glueball content of hadrons in γp interactions at GlueX,” Phys. Rev. D **94** (2016) no.3, 034010 doi:10.1103/PhysRevD.94.034010 [arXiv:1605.01035 [hep-ph]].
- [47] S. Janowski, F. Giacosa and D. H. Rischke, “Is $f_0(1710)$ a glueball?,” Phys. Rev. D **90** (2014) no.11, 114005 doi:10.1103/PhysRevD.90.114005 [arXiv:1408.4921 [hep-ph]].
- [48] W. I. Eshraim, S. Janowski, F. Giacosa and D. H. Rischke, “Decay of the pseudoscalar glueball into scalar and pseudoscalar mesons,” Phys. Rev. D **87** (2013) no.5, 054036 doi:10.1103/PhysRevD.87.054036 [arXiv:1208.6474 [hep-ph]].
- [49] W. I. Eshraim, S. Janowski, A. Peters, K. Neuschwander and F. Giacosa, “Interaction of the pseudoscalar glueball with (pseudo)scalar mesons and nucleons,” Acta Phys. Polon. Supp. **5** (2012) 1101 doi:10.5506/APhysPolBSupp.5.1101 [arXiv:1209.3976 [hep-ph]].
- [50] F. Krinner [for the COMPASS Collaboration], “Light-Meson Spectroscopy at COMPASS,” arXiv:1611.01388 [hep-ex].